









# Combination of T cell-redirecting strategies with a bispecific antibody blocking TGF- $\beta$ and PD-L1 enhances antitumor responses

Antonio Tapia-Galisteo <sup>a,b,c,d</sup>, Iñigo Sánchez-Rodríguez <sup>a\*</sup>, Javier Narbona <sup>e\*</sup>, Patricia Iglesias-Hernández <sup>a</sup>, Saray Aragón-García<sup>a</sup>, Anaís Jiménez-Reinoso <sup>b,c,d</sup>, Marta Compte <sup>f</sup>, Shaukat Khan<sup>g</sup>, Takeshi Tsuda<sup>g</sup>, Patrick Chames <sup>h</sup>, Javier Lacadena <sup>e</sup>, Luis Álvarez-Vallina <sup>b,c,d</sup>, and Laura Sanz <sup>a</sup>

<sup>a</sup>Molecular Immunology Unit, Biomedical Research Institute Hospital Universitario Puerta de Hierro Majadahonda, Madrid, Spain; <sup>b</sup>Cancer Immunotherapy Unit (UNICA), Hospital Universitario 12 de Octubre, Madrid, Spain; <sup>c</sup>Immuno-oncology and Immunotherapy Group, Biomedical Research Institute Hospital 12 de Octubre, Madrid, Spain; <sup>d</sup>H120-CNIO Cancer Immunotherapy Clinical Research Unit, Spanish National Cancer Research Centre (CNIO), Madrid, Spain; <sup>e</sup>Department of Biochemistry and Molecular Biology, Facultad de Ciencias Químicas, Universidad Complutense de Madrid, Madrid, Spain; <sup>f</sup>Department of Antibody Engineering, Leadartis SL, Madrid, Spain; <sup>g</sup>Nemours Children's Health Delaware, Wilmington, Delaware, USA; <sup>h</sup>Aix Marseille Univ, CNRS, INSERM, Institute Paoli-Calmettes, CRCM, Marseille, France

## ABSTRACT

T cell-based immunotherapies for solid tumors have not achieved the clinical success observed in hematological malignancies, partially due to the immunosuppressive effect promoted by the tumor microenvironment, where PD-L1 and TGF- $\beta$  play a pivotal role. However, durable responses to immune checkpoint inhibitors remain limited to a minority of patients, while TGF- $\beta$  inhibitors have not reached the market yet. Here, we describe a bispecific antibody for dual blockade of PD-L1 and TGF- $\beta$ , termed AxF (scFv)<sub>2</sub>, under the premise that combination with T cell redirecting strategies would improve clinical benefit. The AxF (scFv)<sub>2</sub> antibody was well expressed in mammalian and yeast cells, bound both targets and inhibited dose-dependently the corresponding signaling pathways in luminescence-based cellular reporter systems. Moreover, combined treatment with trispecific T-cell engagers (TriTE) or CAR-T cells significantly boosted T cell activation status and cytotoxic response in breast, lung and colorectal (CRC) cancer models. Importantly, the combination of an EpCAM $\times$ CD3 $\times$ EGFR TriTE with the AxF (scFv)<sub>2</sub> delayed CRC tumor growth *in vivo* and significantly enhanced survival compared to monotherapy with the trispecific antibody. In summary, we demonstrated the feasibility of concomitant blockade of PD-L1 and TGF- $\beta$  by a single molecule, as well as its therapeutic potential in combination with different T cell redirecting agents to overcome tumor microenvironment-mediated immunosuppression.

## ARTICLE HISTORY

Received 7 November 2023  
Revised 14 March 2024  
Accepted 30 March 2024

## KEYWORDS



Bispecific antibody; trispecific antibody; T-cell engager; CAR-T cell; cancer immunotherapy; combination therapy; colorectal cancer

## Introduction


Immunotherapy has revolutionized cancer treatment landscape, boosting strong antitumoral responses in patients with advanced tumors. However, the success of immunotherapy in solid tumors has been more limited than in hematological malignancies due to several factors, including the biological complexity of the immunosuppressive tumor microenvironment (TME).<sup>1</sup> Soluble factors (such as TGF- $\beta$ ) and ligands of immune checkpoints, secreted or expressed by stromal or tumor cells, are among major immunosuppressive mechanisms. In particular, the interaction of PD-L1 in the TME with PD-1 expressed by tumor infiltrating lymphocytes promotes an exhausted T cell phenotype, limiting their proliferation rate and effector functions.<sup>2</sup> Interestingly, anti-PD-L1 blockade has also been shown to reinvigorate costimulatory dendritic cell activity over T cells.<sup>3</sup> As of March 2024, ten immune checkpoint inhibitors (ICI) preventing PD1/PD-L1 interaction had been approved by FDA and/or EMA, atezolizumab being the first anti-PD-L1 monoclonal antibody (mAb) in the market. Despite the therapeutic potential of ICI, the TME

orchestrates a complex molecular network that can modulate the susceptibility to anti-PD-(L)1 mAb treatment. Indeed, response rates to a series of cancer such as NSCLC and head and neck, gastroesophageal, and bladder and urothelial cancers are in the range of 15% to 25%,<sup>4</sup> indicating that a significant unmet need remains.

TGF- $\beta$  plays a key role in immunosuppression within the TME, contributing to tumor immune evasion and poor responses to cancer immunotherapy, especially in solid tumors, where enrichment in cancer-associated fibroblast and other tumor stromal cells strongly increases TGF $\beta$  levels in the tumor site.<sup>5-7</sup> In fact, TGF- $\beta$  molecular signature has been associated with resistance to ICI through several pathways, such as blockade of T<sub>H</sub>1 cell phenotype, polarization of immunosuppressor cell populations, including Treg, and effector T cell exclusion.<sup>8-10</sup> In addition, TGF- $\beta$  promotes epithelial-mesenchymal transition (EMT), which enhances tumor proliferation, migration, stemness and chemoresistance.<sup>11</sup> Accumulating evidence suggests that TGF- $\beta$  inhibition can

**CONTACT** Laura Sanz  [lsalcober@salud.madrid.org](mailto:lsalcober@salud.madrid.org)  Molecular Immunology Unit, Biomedical Research Institute Hospital Universitario Puerta de Hierro Majadahonda, Joaquín Rodrigo 2, Madrid 28222, Spain

\*Iñigo Sánchez-Rodríguez and Javier Narbona contributed equally to this work.

 Supplemental data for this article can be accessed online at <https://doi.org/10.1080/2162402X.2024.2338558>

© 2024 The Author(s). Published with license by Taylor & Francis Group, LLC.

This is an Open Access article distributed under the terms of the Creative Commons Attribution-NonCommercial License (<http://creativecommons.org/licenses/by-nc/4.0/>), which permits unrestricted non-commercial use, distribution, and reproduction in any medium, provided the original work is properly cited. The terms on which this article has been published allow the posting of the Accepted Manuscript in a repository by the author(s) or with their consent.

restore cancer immunity and synergize with other immunotherapies, including ICI, to unleash potent immune responses in preclinical cancer models.<sup>7,9,12,13</sup>

Different strategies have been developed to target TGF- $\beta$  mainly in solid tumors<sup>8</sup> with small molecule inhibitors (such as galunisertib) and mAb (such as fresolimumab) being the most advanced approaches in clinical development, although no TGF- $\beta$  inhibitor has been approved for clinical use.<sup>14</sup> Fresolimumab recognizes the three TGF- $\beta$  isoforms with high affinity and has shown a suitable safety profile, but exhibited moderated anti-tumor activity in patients with melanoma and renal cell carcinoma.<sup>15</sup> In general, results of TGF- $\beta$  inhibitors as monotherapy in cancer clinical trials have been inconsistent.<sup>16</sup> In addition, with TGF- $\beta$  being a pleiotropic cytokine crucial for tissue homeostasis, targeting of TGF- $\beta$  has been associated with on-target cardiovascular toxic side effects.<sup>17</sup>

Since TGF- $\beta$  neutralization could improve the susceptibility to PD-(L)1 blockade, combined treatment was an obvious alternative to the use of single-targeted agents. Interestingly, the concomitant therapy with an anti-PD-L1 mAb and an anti-TGF- $\beta$  mAb<sup>12</sup> or a small molecule targeting TGF- $\beta$ <sup>9</sup> facilitated intratumoral CD8<sup>+</sup> and CD4<sup>+</sup> T cell infiltration, and promoted strong immune responses and tumor eradication in breast and colorectal cancer murine models, respectively. An optimized version of fresolimumab, SAR439459, modified for a better manufacturability, triggered complete tumor regression in combination with an anti-PD1 antibody in syngeneic tumor models.<sup>13</sup> However, SAR439459 was discontinued in a clinical trial (NCT03192345) due to insufficient efficacy and bleeding risk.<sup>18</sup> Overall, combination therapies tested in advanced solid tumors showed limited objective responses.<sup>19</sup>

Based on the hypothesis that confining TGF- $\beta$  blockade to the PD-L1-expressing TME compartment could increase anti-tumoral efficacy and decrease potential side effects, we generated a bispecific antibody (bsAb) in tandem scFv (single-chain Fv) or (scFv)<sub>2</sub> format for dual targeting of PD-L1 and TGF- $\beta$ . Such a bsAb could have the potential to enhance the effect of T cell-redirecting immunotherapies. These strategies, which endow T cells with the ability to recognize tumor associated antigens (TAA) and kill cancer cells irrespectively of their TCR specificity, are based on the administration of recombinant T cell engagers (TCE) or the *ex vivo* modification of T cells for the expression of chimeric antigen receptors (CAR-T cells) on their membrane<sup>20</sup> and/or *in vivo* secretion of TCE (STAb-T cells).<sup>21</sup>

Bispecific<sup>22</sup> and trispecific TCE<sup>23</sup> are anti-CD3 fragment-based antibodies able to redirect T cells specifically against one or two TAA and activate them for tumor cell lysis. The first TCE approved by the FDA (2014) was the BiTE<sup>®</sup> blinatumomab, an anti-CD19  $\times$  anti-CD3 tandem scFv with a remarkable clinical success in B cell malignancies.<sup>24,25</sup> From October 2022 to August 2023, the FDA granted approval to six new TCE: the anti-BCMA teclistamab and elranatamab, the anti-CD20 mosunetuzumab, glofitamab and epcoritamab and the anti-GPRC5D talquetamab, all indicated for hematological malignancies,<sup>26</sup> and two more are currently in review. However, there is no TCE approved for the treatment of solid tumors yet,<sup>27</sup> with the exception of the non-canonical fusion protein tebentafusp, highlighting the challenges posed by the paucity of TAA not expressed in essential normal tissues and the immunosuppressive TME.<sup>28</sup> If approved

this year for the treatment of small cell lung cancer, the half-life extended BiTE<sup>®</sup> tarlatamab (DLL3 $\times$ CD3) may be first TCE bsAb for solid tumors.<sup>29</sup> Similarly, CAR-T cell therapies have achieved unprecedented success in the treatment of B cell acute lymphoblastic leukemia, non-Hodgkin lymphoma and multiple myeloma, but no CAR-T cell has reached the market for the treatment of non-hematological malignancies.<sup>30,31</sup>

Here, we show the enhancing effect of a new PD-L1 $\times$ TGF- $\beta$  bsAb on activation of T cells redirected by TCE or *ex vivo* modified CAR-T cells. The bsAb was expressed in a functional state and was able to simultaneously bind to PD-L1 and TGF- $\beta$  and block both signaling pathways. Moreover, a significant increase in IFN- $\gamma$  secretion and lysis of tumor cells was observed *in vitro* when combined with T cells engaged with two different trispecific TCE (EpCAM $\times$ CD3 $\times$ EGFR and HER2 $\times$ CD3 $\times$ EGFR) or anti-EGFR CAR-T cells. Furthermore, increased antitumor efficacy mediated by the EpCAM $\times$ CD3 $\times$ EGFR TriTE was observed when colorectal cancer (CRC) tumor-bearing mice were treated in combination with the PD-L1 $\times$ TGF $\beta$  bsAb. In summary, this combination treatment may improve clinical activity of T cell redirecting strategies in solid tumors and reduce the toxicity related to the administration of anti-PD-L1 and anti-TGF- $\beta$  single agents.

## Materials & methods

### Antibodies

The mAb used included: mouse anti-c-myc clone 9E10 (Abcam, Cambridge, UK), mouse anti-human CD3 $\epsilon$  clone OKT3 (Thermo Fisher Scientific, London, UK), rabbit anti-human N-Cadherin (CST, Danvers, MA), rabbit anti-human E-Cadherin (CST), mouse anti-human EpCAM clone Ber-EP4 (Dako, Agilent, Santa Clara, CA), PE-conjugated anti-human CD69 clone FN50, mouse anti-human CD3 clone OKT3, FITC-conjugated anti-CD3 clone OKT3, mouse anti-CD28 clone CD28.2 (all from BD Biosciences, San Jose, CA), mouse anti- $\beta$ -actin clone 8226 (Abcam) and mouse anti-TGF- $\beta$  1, 2, 3 mAb clone 1D11 (R&D Systems, Minneapolis, MN). Fresolimumab is a humanized version of this mAb. Anti-human EGFR cetuximab, anti-human PD-L1 atezolizumab and anti-human HER2 trastuzumab mAb were obtained from the pharmacy at Hospital Universitario Puerta de Hierro (HUPH). Polyclonal antibodies included: biotinylated anti-human TGF- $\beta$ 1 (R&D Systems), PE-conjugated goat F(ab')<sub>2</sub> fragment anti-mouse IgG, Fc specific, PE-conjugated goat F(ab')<sub>2</sub> fragment anti-human IgG (H&L) (Jackson Immuno Research, Newmarket, UK), horseradish peroxidase (HRP)-conjugated goat anti-mouse IgG, HRP-conjugated goat anti-human IgG (Sigma-Aldrich St Louis, MO), DyLight 800-conjugated anti-mouse IgG (RockLand, Pottstown, PA), IRDye800CW-conjugated donkey anti-rabbit and IRDye680RD-conjugated donkey anti-mouse (LI-COR Biosciences Lincoln, NE).

### Cells and culture conditions

Human 293T (CRL-3216), HCT116 (CCL-247), SKBR3 (HTB-30), A549 (CCL-185) and Jurkat (TIB-152) cell lines were obtained from ATCC. Generation of HCT116, SKBR3 and A549 cell lines expressing the firefly luciferase (Luc) has been described

previously.<sup>11</sup> Peripheral blood mononuclear cells (PBMCs) from healthy donors were provided by the Biobank of HUPH/ Biomedical Research Institute Puerta de Hierro-Segovia de Arana (IDIPHISA) (PT17/0015/0020, Spanish National Biobank Network), with the approval of the Ethics Committee and based on informed consent. Adherent cells, including mink lung epithelial cells (MLEC),<sup>32</sup> were cultured in DMEM medium supplemented with 10% FCS and 1% penicillin/streptomycin/glutamine. Jurkat cells and PBMCs were maintained in RPMI-1640 supplemented as above. All cells were routinely screened for mycoplasma contamination by PCR (Biotools, Madrid, Spain) at the Tissue Culture Core Facility IDIPHISA and were authenticated at the Genomics Unit of Universidad Complutense de Madrid (AmpFLSTR Identifier PCR Amplification kit, Applied Biosystems). *Pichia pastoris* KM71H cells were cultured with YPD (1% yeast extract, 2% peptone, 2% dextrose) or BMXY (1% yeast extract, 2% peptone, 100 mM potassium phosphate buffer pH 6.0,  $4 \times 10^{-5}$  biotin) supplemented with 1% glycerol (BMGY) or 0.5% methanol (BMMY).

### Construction of expression vectors

To generate the anti-PD-L1 and the anti-TGF- $\beta$  scFv, the sequences encoding the VH and VL domains of atezolizumab and fresolimumab IgG, respectively, were obtained from the Drugbank database and fused by a 15-mer linker. Both scFv were joined by a 5-mer linker, and the sequence was synthesized by GeneArtAG (Thermo Fisher Scientific) and subcloned into a pCR3.1 backbone. For medium scale protein production, the AxF (scFv)<sub>2</sub> construct was subcloned into the pPicza vector (Invitrogen). All plasmids were amplified in chemically competent *Escherichia coli* TOP10 and purified using Qiagen (Hilden, Germany) plasmid Midi kit.

### Expression in mammalian cells

293T cells were transiently transfected with pCR3.1 vectors encoding the Atezo scFv, Freso scFv or AxF (scFv)<sub>2</sub> using calcium phosphate and conditioned media (CM) were collected after 48 h. Antibody expression was analyzed using ELISA and Western Blotting.

### Expression in *P. pastoris* and purification of recombinant antibodies

Linearized pPicza-AxF (scFv)<sub>2</sub> plasmid was electroporated in electrocompetent *P. pastoris* KM71H strain cells using Bio-Rad (Hercules, CA) Gene pulser apparatus. Yeast cells were selected in YPD plates with zeocin and protein expression was induced using BMMY (buffered media for yeast containing methanol 0.5% v/v) as previously described.<sup>22</sup> The AxF (scFv)<sub>2</sub> was purified by affinity chromatography with HisTrap<sup>TM</sup> HP columns (GE Healthcare, Uppsala, Sweden) using an ÄKTA Prime plus system (GE Healthcare). Endotoxin levels were <0.25 EU/ml as determined by the LAL Endotoxin Kit (Pierce).

### Size exclusion chromatography

Purified AxF (scFv)<sub>2</sub> was injected into a Superdex 200 Increase 10/300 GL column (Cytiva, MA, US) on an ÄKTA GO chromatography system (Cytiva) at room temperature, while monitoring light absorbance at 280 nm. The column was equilibrated in PBS pH 7.4 plus 150 mM NaCl and run in the same buffer at 0.5 ml per minute. The column was previously calibrated with a set of Gel Filtration Standards (Biorad, from 1.4 to 670 kDa).

### Circular dichroism

Circular dichroism measurements were performed with a Jasco J-810 spectropolarimeter (JASCO, Tokyo, Japan). The spectra were recorded on protein samples at 0.2 g/L in PBS using 0.2 cm path length quartz cuvettes at 25°C.

### Western blot

Cell-free CM containing the proteins or the purified AxF (scFv)<sub>2</sub> antibody were analyzed under reducing conditions on 12% Tris-glycine gels. After transference to nitrocellulose membranes using iBlot system (Life Technologies, California, US) and incubation with LI-COR blocking solution, proteins were detected with 1  $\mu$ g/mL anti-c-myc mAb. Subsequently, the membranes were incubated with DyLight800-conjugated goat anti-mouse IgG (1:5000 dilution) and the visualization of protein bands was performed with the Odyssey system (LI-COR Biosciences).

### Enzyme-linked immunosorbent assay

Maxisorp plates (Nunc Brand Products) coated with 5  $\mu$ g/mL human PD-L1-Fc or human TGF- $\beta$ 1 were blocked with PBS 5% BSA, followed by an incubation with CM or serial dilutions of purified AxF (scFv)<sub>2</sub> for 1 h at room temperature. After washing, wells were incubated with anti-c-myc mAb (1  $\mu$ g/mL) for 1 h at room temperature and recombinant antibodies were detected with HRP-conjugated goat-anti-mouse IgG (1:1000 dilution) for 45 min at room temperature. Finally, the plates were developed using OPD in citrate phosphate buffer and the reaction was stopped using sulfuric acid 1 M. Atezolizumab and 1D11 IgG (5  $\mu$ g/ml) were used as positive controls and detected with HRP-conjugated goat-anti-human IgG (1:1000 dilution) or HRP-conjugated goat-anti-mouse IgG (1:1000 dilution), respectively.

### Simultaneous binding assessed by two-step sandwich ELISA

Human PD-L1-Fc chimera was immobilized (5  $\mu$ g/ml) on Maxisorp plates overnight at 4°C. After washing and blocking with PBS 5% BSA for 1 h at 37°C, serial dilutions of AxF (scFv)<sub>2</sub> were added for 1 h at room temperature. After a series of washes, wells were incubated with biotinylated TGF- $\beta$  (2  $\mu$ g/ml) for 1 h at room temperature. Wells were again washed and subsequently incubated with HRP-conjugated streptavidin (1:10.000 dilution) for 45 min at room temperature. Finally, OPD was added and the reaction was stopped using sulfuric acid 1 M.



### Flow cytometry

For titration experiments, CHO<sup>PD-L1</sup> cells were incubated with tenfold dilution series of AxF (scFv)<sub>2</sub> ranging from 100 nM to 1 pM for 1 hour at 4°C. After washing, the antibody was detected with anti-c-myc mAb (1 µg/ml), followed by (PE)-conjugated goat-anti-mouse antibody (1:200 dilution) for 30 min at 4°C. Atezolizumab was used as a positive control. To analyze the expression profile of EGFR, EpCAM, HER2 or PD-L1 on the cell surface, CHO, CHO<sup>PD-L1</sup>, HCT116, SKBR3 or A549 were stained with cetuximab (1 µg/ml), anti-EpCAM clone Ber-EP4 (1:200 dilution), trastuzumab (1 µg/ml) or atezolizumab (1 µg/ml), respectively, and detected using a PE-conjugated goat-anti-human antibody (1:50 dilution) or a PE-conjugated goat-anti-mouse antibody (1:200 dilution). Cells incubated with secondary antibodies were used as negative controls. Samples were acquired on a MACSQuant Analyzer 10 (Miltenyi Biotec, Bergisch Gladbach, Germany) and analyzed using FlowJo (BD Biosciences) at the Flow Cytometry Core Facility, IDIPHISA.

### Serum stability

Purified AxF (scFv)<sub>2</sub> (6 µg) was incubated in PBS 60% human or mouse serum at 37°C for 5 days. Samples (1 µg) were collected at 3 h and every 24 h until day 4, and their binding activities were tested by ELISA, representing the sample at 0 h 100% of functionality.

### TGF-β neutralizing activity

Mink lung epithelial cells (MLEC), transfected in a stable way with a PAI-1 promoter-Luciferase construct,<sup>32</sup> were plated in triplicates ( $4 \times 10^4$  cells/w) into microtiter 96-well plates and incubated for 24 h at 37°C. Then, cells were treated with DMEM containing 10 ng/ml of TGF-β and serial dilutions of the AxF (scFv)<sub>2</sub> antibody for 20 h at 37°C. Then, culture medium was replaced by PBS containing 20 µg of D-luciferin (Promega) and the TGF-β neutralizing activity of AxF (scFv)<sub>2</sub> was measured with the luminescence plate reader Infinite 1200 (Tecan, Männedorf, Switzerland). TGF-β receptor inhibitor SB431542 or anti-TGF-β clone 1D11 IgG were used as positive controls of TGF-β blockade and cells only treated with TGF-β as a positive control of stimulation. This MLEC-based bioassay was also used to quantify TGF-β in CM of the three tumor cell lines as previously described.<sup>32</sup> A standard curve with different concentrations of human recombinant TGF-β1 was obtained at each experiment.

### Effect of PD-L1×TGF-β bispecific antibody on TGF-β-induced gene expression

Human brain vascular pericytes (HBVP) were seeded ( $1 \times 10^5$  cells/w) into 12-well plates and treated with TGF-β (10 ng/ml) and AxF (scFv)<sub>2</sub> (50 nM) for 24 h at 37°C. Total RNA was isolated using RNeasy Micro Kit (Qiagen). Synthesis of cDNA from 500 ng of total RNA was performed by random primed reverse transcription with NZY First-Strand cDNA Synthesis Kit (Nzytech, Lisboa, Portugal). Expression of selected genes was determined by quantitative real-time PCR (qRT-PCR) using specific primers obtained from Roche Diagnostics<sup>11</sup> and the Lightcycler 480 apparatus. Fold-

expression changes were calculated using the equation  $2^{-(\Delta\Delta C_t)}$ , as previously described.<sup>11</sup> Samples were tested in triplicates. To study modulation of EMT markers, 6-well plates were seeded with A549 ( $1 \times 10^5$  cells/w) for 24 h and starved in DMEM 0.1% FCS for 5 h. Then, cells were stimulated with 10 ng/ml human TGF-β1 in the presence of AxF (scFv)<sub>2</sub> or 1D11 IgG (both 100 nM) for 72 h. Expression of N-Cadherin and E-Cadherin was determined by western blotting using 1 µg/ml of each mAb, and detected with 1:5000 IRDye800CW-donkey anti-rabbit Ab. Anti-β-actin mouse clone 8226 (2 µg/ml) detected with 1:5000 IRDye680RD-donkey anti-mouse was used as loading control. In T cell experiments,  $1 \times 10^6$  preactivated cells were seeded into 12-well plates and treated with TGF-β (10 ng/ml) and AxF (scFv)<sub>2</sub> or 1D11 (50 nM) for 24 h at 37°C.

### PD-1/PD-L1 neutralizing activity by PD-1/PD-L1 blockade bioassay

The luciferase reporter assay (PD-1/PD-L1 Blockade Bioassay, Promega) was performed according to the manufacturer's instructions. Microtiter 96-well plates were seeded with aAPC/CHO-K1<sup>PD-L1</sup> cells ( $3 \times 10^4$  cells/w). After incubation for 20 h at 37°C, ten-fold serial dilutions of the AxF (scFv)<sub>2</sub> or atezolizumab antibodies were added, followed by Jurkat<sup>PD-1</sup> cells ( $15 \times 10^4$  cells/w). After 6 h of coculture at 37°C, Bio-Glo Luciferase Assay Reagent (Promega) was added and luciferase activity was analyzed using the Infinite luminometer.

### CAR-EGFR vector generation, lentivirus production and T cell transduction

To generate the lentiviral transfer vector, the anti-EGFR V<sub>HH</sub> Ega1 gene<sup>33</sup> was synthesized by GeneArt and cloned into the vector pCCL-EF1a-CAR-CD1a-T2A-GFP,<sup>34</sup> encoding a second-generation (CD8-41BB-CD3ζ) CAR, to obtain the plasmid pCCL-EF1a-CAR-Ega1-T2A-GFP. CAR-expressing viral particles pseudotyped with VSV-G were generated by transfection of 293T cells using polyethylenimine and a third-generation plasmid system comprising pMDLg/pRRRE, pRSVrev and envelope pMD2.G plasmids. Supernatants were collected 48 h after, concentrated by ultracentrifugation and titrated. Microtiter 96-wells were coated with anti-human CD3/anti-human CD28 antibodies (1 µg/ml) for 3 h at 37°C. Then, PBMC from healthy donors were isolated using Lymphoprep and seeded at a concentration of  $1 \times 10^6$  cells/ml. After activation and expansion for 24 h in the presence of IL-7 and IL-15 (10 ng/ml), cells were transduced with lentiviral particles encoding CAR-EGFR at MOI of 10. Non-transduced cells (N-T T cells) were used as a negative control.

### T cell activation assays

Microtiter 96-well plates were seeded with HCT116, SKBR3 (both at  $2 \times 10^4$ /well) or A549 ( $1 \times 10^4$ /well) cell lines. After 24 h, wells were incubated with increasing amounts of two trispecific T-cell engagers in TriTE format, the EpCAM×CD3×EGFR (named AxOxE)<sup>23</sup> or HER2×CD3×EGFR (named CxOxE) TriTE, with or without 100 nM AxF (scFv)<sub>2</sub> for 30 min at

37°C. After washing, human PBMC were added at 5:1 effector:target (E:T) ratio. After 24 h, the expression profile of the activation marker CD69 was determined by flow cytometry using PE-conjugated anti-CD69 mAb and FITC-conjugated anti-CD3 mAb incubated for 30 min on ice. Samples were analyzed with a MACSQuant Analyzer 10.

### Cytotoxicity assays

HCT116<sup>Luc</sup>, SKBR3<sup>Luc</sup> or A549<sup>Luc</sup> cells were seeded in triplicates in 96-well microtiter plates for 24 h. In TriTE-based experiments, tumor cells were incubated with increasing amounts of purified HER2×CD3×EGFR or EpCAM×CD3×EGFR TriTE and 100 nM of AxF (scFv)<sub>2</sub> for 30 min at 37°C. Then, human PBMCs were added at 5:1 E:T ratio. Wells with target and effector cells in the absence of purified antibodies were set as 100% viability. In single concentration experiments, tumor and T cells were incubated with 10 pM of EpCAM×CD3×EGFR TriTE and 100 nM of AxF (scFv)<sub>2</sub>, atezolizumab or 1D11 IgG. In CAR-EGFR T cell-based experiments, tumor cells were cocultured with CAR-EGFR or N-T T cells at different E:T ratios in the presence of 100 nM AxF (scFv)<sub>2</sub>. Wells with target cells and N-T T cells in the absence of AxF (scFv)<sub>2</sub> were set as 100% viability. After 48 h, specific cytotoxicity was quantified adding 20 µg/well D-luciferin substrate and measured with the luminescence plate reader. CM were collected and assayed for IFN-γ by ELISA (Diacclone, Besançon, France) following manufacturer's instructions.

### In vivo antitumoral efficacy

HCT116 (2 × 10<sup>6</sup> cells/mouse) in PBS mixed with 30% matrigel (BD Biosciences) were implanted subcutaneously (s.c.) into the right dorsal space of 5-week-old female Hsd:Athymic Nude-Foxn1<sup>nu</sup> mice. At day 3, mice were randomized into groups with average diameter of 0.3 cm and inoculated i.p. with 1 × 10<sup>7</sup> PBMCs from a healthy donor. PBS and AxOxE TriTE (4 mg/kg) were administered i.p. daily for 7 days, and AxF (scFv)<sub>2</sub> (3 mg/kg) for 6 days, starting 1 day after the first dose of AxOxE TriTE. Daily administration of the recombinant antibodies was based on their small size and short half-life. Atezolizumab was used as a control with i.p. injections of 100 µg at day 5 and 10. Tumors were measured three times a week and their volumes estimated by using the formula: length × width<sup>2</sup> × 0.52. Mice were euthanized when tumor size reached a volume of 0.8 cm<sup>3</sup> or at the onset of any sign of distress. All experiments were conducted in compliance with the institutional guidelines provided by the HUPH/IDIPHISA Animal Ethics Committee. Procedures were additionally approved by the Animal Welfare Division of the Environmental Affairs Council, Comunidad Autónoma de Madrid (PROEX 066/14).

### Statistical analysis

Results were showed as mean ± standard deviation (SD). Data were analyzed by unpaired two-tailed Student's t-test, assuming a normal distribution, using Prism software v5 (GraphPad, San Diego, CA, USA). Data were considered statistically significant when *p* < 0.05.

## Results

### Design and expression of a PD-L1×TGF-β bispecific tandem scFv antibody

To generate the bsAb, we designed scFv derived from the anti-PD-L1 mAb atezolizumab and the anti-TGF-β mAb fresolimumab and fused them with a five-amino acid (G<sub>4</sub>S) linker in a single polypeptide chain, hereafter referred to as AxF (scFv)<sub>2</sub> (Figure 1a). Western blot analysis of conditioned media (CM) from 293T cells transfected with the AxF (scFv)<sub>2</sub> showed a migration pattern consistent with the calculated molecular weight, around 55 kDa (Supplementary Figure S1A). The AxF (scFv)<sub>2</sub> was able to bind both antigens immobilized on plastic by ELISA (Supplementary Figure S1B) and PD-L1 expressed on the membrane of stably transfected CHO<sup>PD-L1</sup> cells. However, no binding was detected when the recombinant antibody was incubated with wild-type CHO cells (Supplementary Figure S1C).

### Purification and characterization of the PD-L1×TGF-β bispecific antibody

Then, the sequence encoding AxF (scFv)<sub>2</sub> was subcloned in the pPICZα vector and electroporated in *P. pastoris* cells. After 48 h of methanol induction, the protein was purified by IMAC, with a yield of 2.5 mg/L of induction medium. SDS-PAGE analysis of the purified antibody showed a single band (>95% pure) with the expected molecular weight (Figure 1b). Accordingly, size exclusion chromatography (SEC) analysis revealed a single peak in the volume corresponding to the monomeric globular structure of 55 kDa (Figure 1c). The circular dichroism spectrum of AxF (scFv)<sub>2</sub> (Figure 1d) was typical of proteins with predominant β-sheet structure.

Functionally, the AxF (scFv)<sub>2</sub> showed dose-dependent binding curves against plastic-immobilized PD-L1 and TGF-β by ELISA (Figure 1e), as well as PD-L1 expressed on the cell surface of CHO<sup>PD-L1</sup> cells by flow cytometry (Figure 1f). Importantly, AxF (scFv)<sub>2</sub> was able to bind simultaneously both targets, as assessed by two-step sandwich ELISA (Figure 1g), demonstrating that interactions with the two antigens were sterically compatible.

Long-term stability of the AxF (scFv)<sub>2</sub> incubated in 60% mouse or human serum for 4 days at 37°C was analyzed. The recombinant protein was able to retain 90% of its binding activity to PD-L1 after 96 h of incubation, showing its high stability and resistance to the proteolytic activity of serum proteases (Figure 1h).

### Inhibition of the TGF-β signalling pathway by the PD-L1×TGF-β bispecific antibody

The ability of the AxF (scFv)<sub>2</sub> to block TGF-β/TGF-βR interaction was assessed using a mink lung epithelial cell (MLEC)-based reporter system, with luciferase expression driven by the PAI promoter, conditionally activated by TGF-β.<sup>32</sup> MLEC cells were treated with 10 ng/mL TGF-β and serial dilutions of purified AxF (scFv)<sub>2</sub> or the anti-TGF-β IgG 1D11, both ranging from 100 to 0.4 nM. Treatment with the bsAb promoted a dose-dependent inhibition of luciferase expression, with an IC<sub>50</sub> value of 2.6 nM,

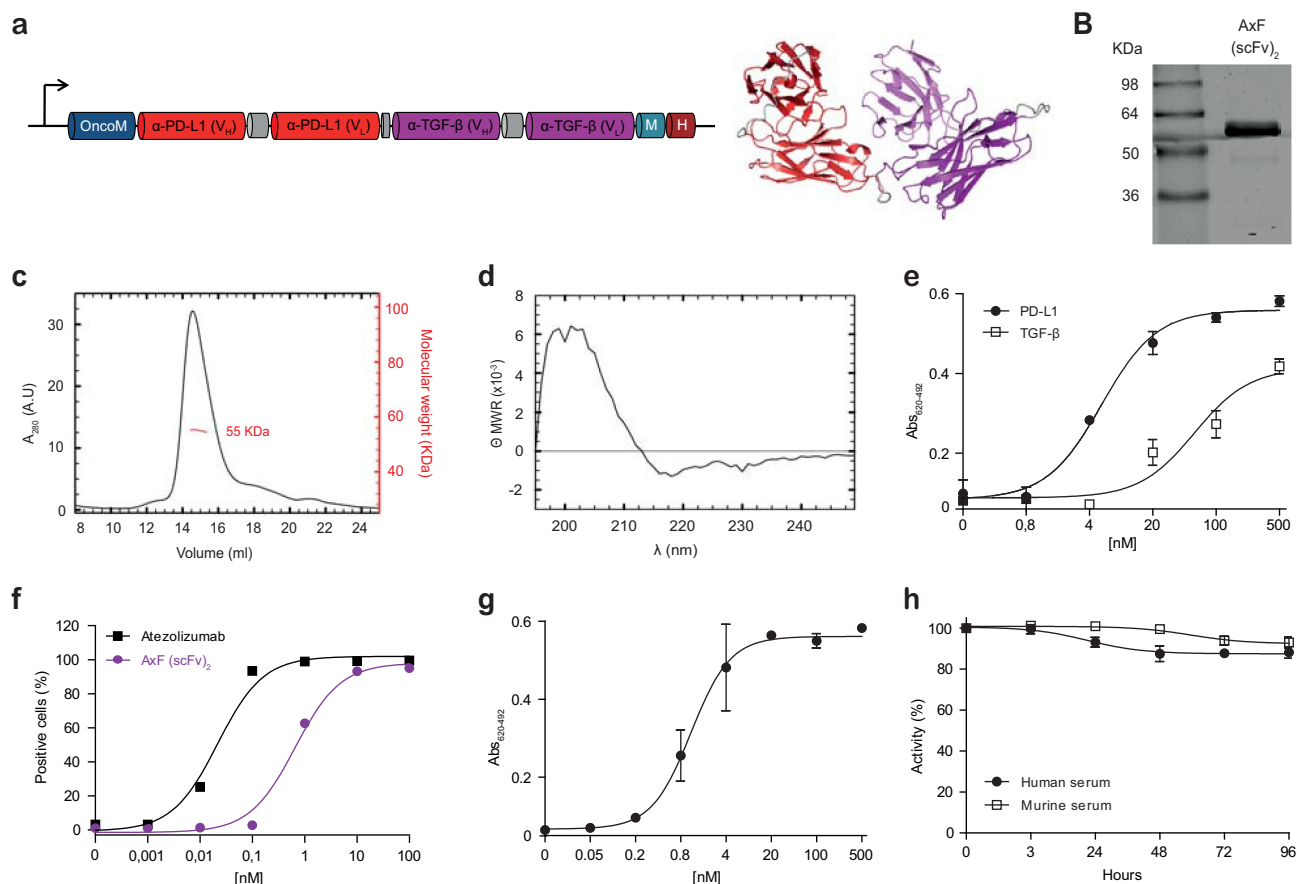


**Figure 1.** Structural and functional characterization of the PD-L1×TGF- $\beta$  bispecific antibody. (a) Genetic structure of the tandem scFv anti-PD-L1  $\times$  anti-TGF- $\beta$  named AxF (scFv)<sub>2</sub>. Oncostatin M signal peptide is used to direct the secretion of the recombinant antibody, and the myc/6 $\times$ His tags (light blue and dark red boxes) were appended for immunodetection and affinity purification, respectively. A 3D model of AxF (scFv)<sub>2</sub> was built with AlphaFold and refined using Pymol. (b) Reducing SDS-PAGE of the construct, (c) size exclusion chromatography analysis with the indicated molecular weight measured at the center of the chromatography peak (red line) and (d) circular dichroism analysis of the purified AxF (scFv)<sub>2</sub>. (e) ELISA titration against plastic-immobilized human PD-L1 or TGF- $\beta$  of the purified AxF (scFv)<sub>2</sub> and (f) dose-dependent binding curve to the CHO<sup>PD-L1</sup> cell surface by FACS. (g) Simultaneous binding of the recombinant antibody to PD-L1 and TGF- $\beta$  by two-step ELISA. (h) Serum stability of the AxF (scFv)<sub>2</sub> incubated in mouse or human serum for 96 hours.

demonstrating strong blockade of the TGF- $\beta$  axis (Figure 2a). These results confirmed preliminary data with CM from 293T expressing AxF (scFv)<sub>2</sub>, which decreased light emission nearly to background levels, effect comparable to that observed with 5  $\mu$ g/ml of the TGF- $\beta$ R1 kinase inhibitor SB431542 (Supplementary Figure S1D).

To analyze the biological effect of TGF- $\beta$ /TGF- $\beta$ R pathway disruption, the expression profile of several TGF- $\beta$ -inducible genes was assessed in human pericytes.<sup>11</sup> RT-qPCR analyzes showed that treatment with AxF (scFv)<sub>2</sub> significantly inhibited expression of a series of genes stimulated with TGF- $\beta$ , including *IGFBP3* ( $p < 0.0001$ ), *VCAN* ( $p < 0.001$ ) and *SMAD7* ( $p < 0.0001$ ) (Figure 2b). In  $\alpha$ CD3/ $\alpha$ CD28-activated T cells, AxF (scFv)<sub>2</sub> also reversed *PDCD1* overexpression promoted by TGF- $\beta$  ( $p = 0.004$ ) as assessed by RT-qPCR (Figure 2c).

In addition, TGF- $\beta$  is well known to promote the EMT, which has been widely associated to increased invasiveness and tumor progression.<sup>10</sup> Therefore, we proceeded to investigate whether AxF (scFv)<sub>2</sub> could modulate the expression of EMT markers as assessed by WB. Interestingly, the AxF (scFv)<sub>2</sub> was able to block up to 74% upregulation of the mesenchymal marker N-cadherin promoted by 10 ng/ml of TGF- $\beta$ , and completely inhibited the downregulation of the epithelial marker E-cadherin (Figure 2d).

### Inhibition of PD1/PD-L1 axis by the PD-L1×TGF- $\beta$ bispecific antibody

Next, we assessed the capability of AxF (scFv)<sub>2</sub> to block the PD-1/PD-L1 pathway using a luciferase-based reporter system. Jurkat<sup>PD-1</sup> reporter cells were cocultured with aAPC/CHO-K1<sup>PD-L1</sup> cells in the presence of increasing amounts of the AxF (scFv)<sub>2</sub>, atezolizumab or trastuzumab (0–50 nM). While treatment with trastuzumab showed no effect in the PD-1/PD-L1 axis activity, both AxF (scFv)<sub>2</sub> and atezolizumab IgG triggered a dose-dependent inhibition of that interaction, leading to NFAT activation and light emission (Figure 2e).

### Combination of the PD-L1×TGF- $\beta$ bispecific antibody and trispecific TCE promoted T cell activation and lysis of cancer cells

We next assayed whether the AxF (scFv)<sub>2</sub> could enhance the antitumor activity promoted by two different TriTE.<sup>23</sup> For this purpose, PBMC from three healthy donors were cocultured with TGF- $\beta$ -secreting tumor cell lines expressing different levels of PD-L1, EGFR, HER2 and EpCAM (Supplementary Figure S2A and 2B) at a 5:1 effector to

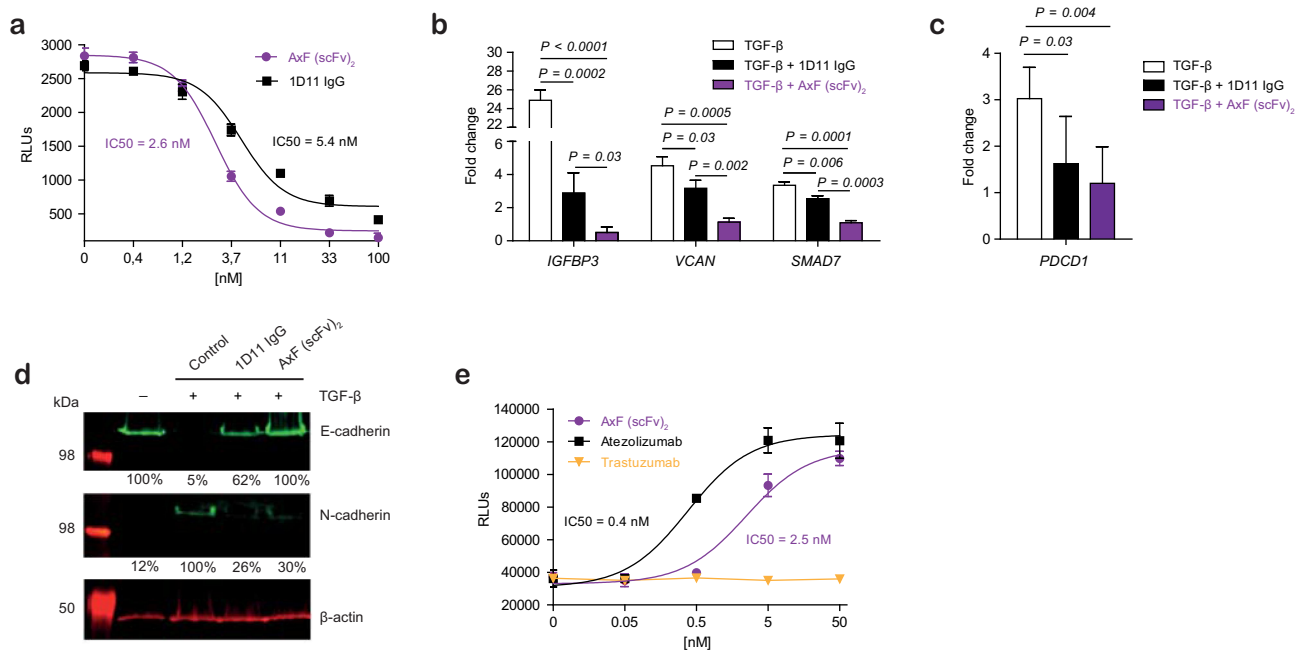


**Figure 2.** Disruption of PD-L1 and TGF- $\beta$  signaling axes promoted by purified PD-L1 $\times$ TGF- $\beta$  bispecific antibody. (a) Dose-dependent blockade of TGF- $\beta$ /TGF- $\beta$ R interaction triggered by the AxF (scFv)<sub>2</sub> using a mink lung epithelial cell (MLEC)-based reporter system. 1D11 IgG was used as a control. (b) Suppression of TGF- $\beta$ -dependent gene expression in human pericytes treated with TGF- $\beta$  in the presence of AxF (scFv)<sub>2</sub>, as assessed by qRT-PCR. (c) TGF- $\beta$ -mediated increase of *PDCD1* gene expression in T cells is reversed by AxF (scFv)<sub>2</sub> and anti-TGF- $\beta$  1D11 IgG. Experiments were performed at least twice in triplicates. (d) Modulation of E- and N-cadherin expression in A549 cells treated with TGF- $\beta$  in the presence of the AxF (scFv)<sub>2</sub>. (e) Inhibition of PD-1/PD-L1 axis by the AxF (scFv)<sub>2</sub> as assessed with a luciferase-based reporter bioassay. Statistical differences were examined by unpaired Student's t-test assuming a normal distribution. Mean  $\pm$  SD are shown at each condition.

target (E:T) ratio. Cocultures were treated with a concentration range of TriTE (from 0 to 100 nM), in the presence or not of 100 nM AxF (scFv)<sub>2</sub>. The trispecific constructs used in these experiments were an anti-EpCAM (clone A2)  $\times$  anti-CD3 (clone OKT3)  $\times$  anti-EGFR (clone EGa1), abbreviated as AxOxE TriTE,<sup>23</sup> and a previously unpublished anti-HER2 (clone CE4)  $\times$  anti-CD3  $\times$  anti-EGFR (Supplementary Figure S3), named CxOxE TriTE. As shown in Figure 3a, while both TriTE triggered dose-dependent T cell activation against target cells, the combination with the AxF (scFv)<sub>2</sub> could decrease up to 3-fold the EC<sub>50</sub> value. In HCT116, cotreatment with AxF (scFv)<sub>2</sub> doubled the number of CD69<sup>+</sup> T cells stimulated with 1 nM AxOxE TriTE. Furthermore, the combined treatment increased the cytotoxic response against HCT116 tumor cells more than 34-fold after 48 h of coculture, with EC<sub>50</sub> values of 0.6 pM vs 20.8 pM for monotherapy with AxOxE TriTE ( $p = 0.03$ ) (Figure 3b). The increase in cytotoxic activity of T cells stimulated with AxOxE or CxOxE TriTE against A549 or SKBR3 cells was also statistically significant ( $p = 0.045$  and  $p = 0.034$ , respectively). These results showed the enhancing effect of the dual blockade of PD-L1 and TGF- $\beta$  on TriTE-mediated antitumoral response. Interestingly, the effect of AxF (scFv)<sub>2</sub> was superior to that of control 1D11 and atezolizumab at equimolar concentrations (Supplementary Figure S4).

In agreement with the previous data, the combined treatment also elicited a stronger IFN- $\gamma$  secretion, increasing the levels of the cytokine up to 30% at the highest dose in cocultures with HCT116 and up to 20% with SKBR3 (Figure 3c).

### Combination of PD-L1 $\times$ TGF- $\beta$ bispecific antibody and anti-EGFR CAR-T cells promoted lysis of EGFR<sup>+</sup>PD-L1<sup>+</sup> cancer cells

To determine if the effect of the dual blockade of PD-L1 and TGF- $\beta$  promoted by the AxF (scFv)<sub>2</sub> could be extensible to other T cell-based cancer immunotherapies, its combination with CAR-T cells was also studied. For this purpose, an anti-EGFR Ega1-based second generation CAR (referred to as CAR-EGFR) was designed (Supplementary Figure S5A) and T cells were transduced with lentiviral particles at MOI of 10. Transduction efficiency was determined after 6 days by flow cytometry based on GFP<sup>+</sup>CAR<sup>+</sup>CD3<sup>+</sup> phenotype. Lentivirus-transduced CAR-EGFR primary T cells showed a higher proportion of CD8<sup>+</sup> than CD4<sup>+</sup> T cells (Supplementary Figure S5B). CAR-EGFR T cells were efficiently activated in the presence of immobilized EGFR, EGFR-coated beads or EGFR<sup>+</sup> target cells (Supplementary Figure S5C).

HCT116 or SKBR3 tumor cells were cocultured with non-transduced T cells (N-T T cells) or CAR-EGFR T cells at different effector:target (E:T) ratios, in the presence or not of the AxF (scFv)<sub>2</sub>. Interestingly, a 70% of specific lysis against HCT116 tumor cells was triggered by CAR-EGFR T cells combined with the AxF (scFv)<sub>2</sub> at the highest E:T ratio, compared to the 50% reached by the CAR-EGFR T cells alone ( $p = 0.0009$ ) (Figure 4a). Moreover, the addition of the bsAb decreased 10-fold the number of CAR-EGFR T cells required to kill the 50% of SKBR3 tumor cells ( $p = 0.042$ ) (Figure 4b). As expected, no cytotoxic effect was observed when N-T T cells were cocultured with target tumor cells at the highest E:T ratio, independently of the presence of the AxF (scFv)<sub>2</sub>. Treatment with the AxF (scFv)<sub>2</sub> also promoted efficiently IFN- $\gamma$  secretion by CAR-EGFR T cells, as shown in Figure 4c,d.



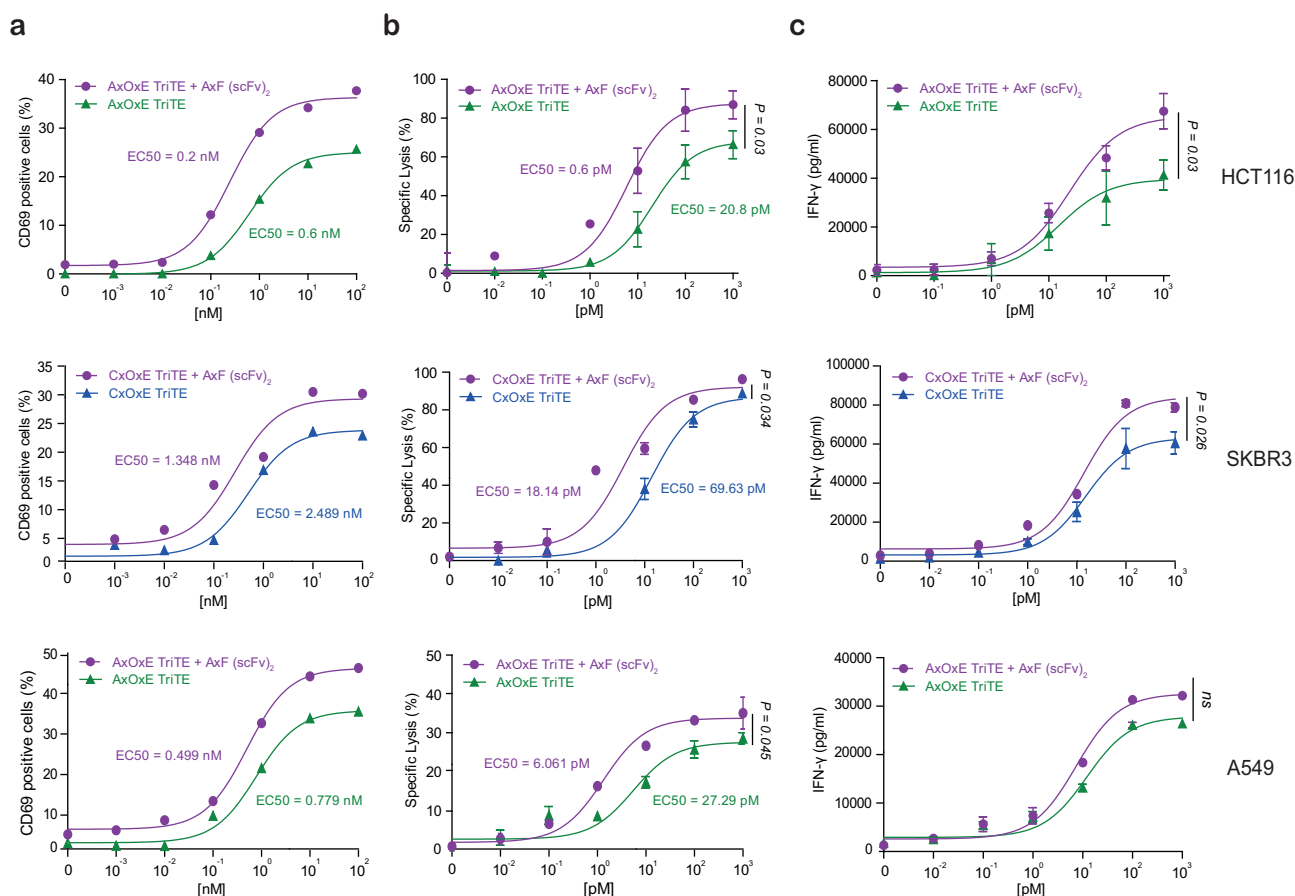


**Figure 3.** TriTE-mediated T cell activation, cytotoxicity and IFN- $\gamma$  secretion is enhanced by purified PD-L1 $\times$ TGF- $\beta$  bispecific antibody. A549, HCT116 or SKBR3 cells were cocultured in 96-well plates with PBMCs at the effector/target (E:T) ratio of 5:1 in the presence of different concentrations of purified TriTE antibodies and 100 nM of AxF (scFv)<sub>2</sub>. (a) Expression of T cell activation marker CD69 at 24 hours, determined by FACS analysis. (b) Specific cytotoxicity of tumor cells as assessed by bioluminescence. Percent specific lysis was calculated relative to an equal number of tumor cells cultured with PBMCs in the absence of purified antibodies. EC50 values are provided according to the color code. (c) IFN- $\gamma$  production was determined in CM by ELISA. PBMCs were obtained from 3 different donors, and experiments were performed in triplicate. Results are expressed as a mean  $\pm$  SD.

### ***In vivo* effect of the TriTE EpcAM $\times$ CD3 $\times$ EGFR in combination with PD-L1 $\times$ TGF- $\beta$ bispecific antibody**

To study the therapeutic effect of combined treatment *in vivo*,  $2 \times 10^6$  HCT116 cells were implanted in Hsd:Athymic Nude-Foxn1<sup>tmu</sup> mice, followed 3 days later by intraperitoneal (i.p.) administration of  $1 \times 10^7$  PBMC. Treatment with AxOxE TriTE, AxF (scFv)<sub>2</sub> or a combination of AxOxE TriTE plus AxF (scFv)<sub>2</sub> was initiated when the tumors reached diameters of 0.3 cm. Equimolar doses of the antibodies (3 mg/kg for AxF (scFv)<sub>2</sub> and 4 mg/kg for AxOxE TriTE) were administered i.p. daily for 7 days (Figure 5a). Atezolizumab (100  $\mu$ g/mice) was administered at days 5 and 10. While mice receiving PBS had been all euthanized at day 29 after tumor implantation, mice treated only with AxOxE TriTE showed a significant delay in tumor growth (Figure 5b). As expected, the AxF (scFv)<sub>2</sub> by itself did not exert a remarkable effect. However, the combination significantly decreased tumor growth and increased survival compared to the AxOxE TriTE group ( $p = 0.003$ ) (Figure 5c). Importantly, whereas 50% of AxOxE TriTE-treated mice had been sacrificed at day 43 after tumor cell implantation, all the mice receiving the combination treatment were still alive, and 50% survived beyond day 53 post-inoculation.

### **Discussion**

Currently, there is no TCE or CAR-T cell strategy approved for the treatment of solid tumors. Undoubtedly, this is due to a plethora of factors, including the difficulty to find target antigens with a favorable safety profile. On the other hand, T cells activated by TCE or armed with CAR will eventually face the same risk of exclusion and/or exhaustion due to the hostile TME in solid tumors than T cells of untreated patients, and additional strategies to revert immunosuppression are needed. TGF- $\beta$  is a pleiotropic cytokine that can play a suppressive or pro-tumorigenic role depending on the tumor stage.<sup>35</sup> Moreover, it has been reported that the TGF- $\beta$  signature promotes anti-PD-L1 therapy resistance.<sup>9</sup> For example, PSMA-targeting CAR-T cells armored with a dominant negative TGF- $\beta$  receptor have demonstrated promising efficacy in a phase 1 trial with prostate cancer patients.<sup>36</sup>

Here, we characterize an anti-PD-L1  $\times$  anti-TGF- $\beta$  bsAb in tandem scFv format, which can simultaneously block both targets. The dose-dependent disruption of the TGF- $\beta$  axis by the bsAb was demonstrated in a luminescence-based cellular reporter system, resulting in strong blockade of TGF- $\beta$ -driven gene transcription, as well as in efficient downregulation of key



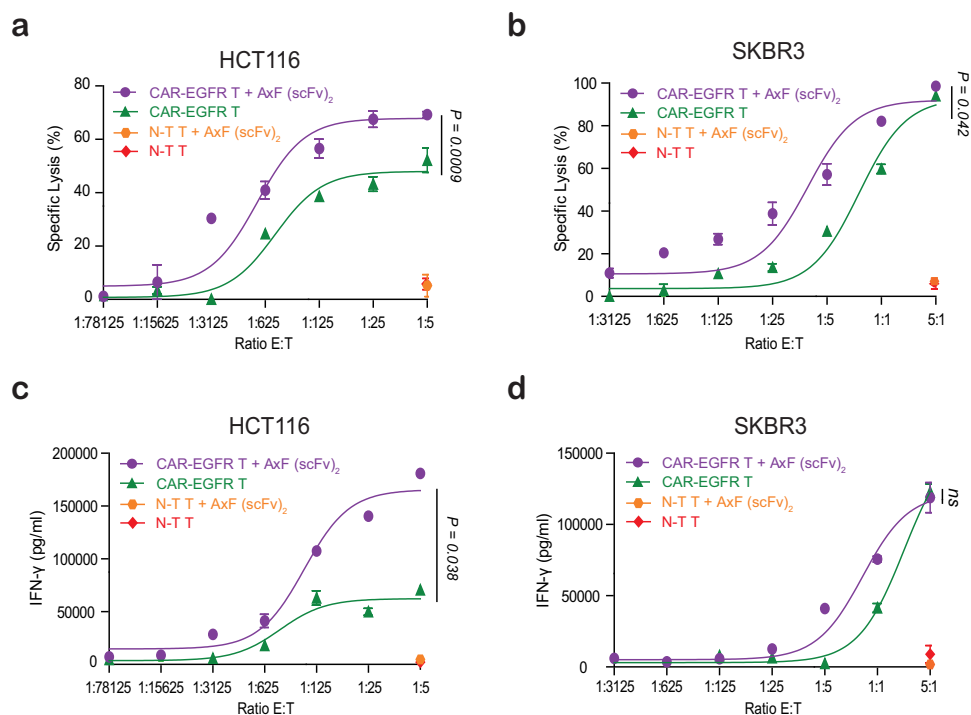


**Figure 4.** Cytotoxicity and IFN- $\gamma$  secretion elicited by CAR-T cells improved by purified PD-L1 $\times$ TGF- $\beta$  bispecific antibody. HCT116 or SKBR3 cells were cocultured in 96-well plates CAR-EGFR or non-transduced (N-T) T cells at different E:T ratios in the presence of 100 nM of AxF (scFv)<sub>2</sub>. (a, b) After 48 hours, specific cytotoxicity of tumor cells were measured by bioluminescence assay. Percent specific lysis was calculated relative to an equal number of tumor cells cultured with N-T T cells in the absence of AxF (scFv)<sub>2</sub>. (c, d) IFN- $\gamma$  secretion was determined in CM by ELISA. PBMCs were obtained from 3 different donors, and experiments were performed in triplicate. Results are expressed as a mean  $\pm$  SD.

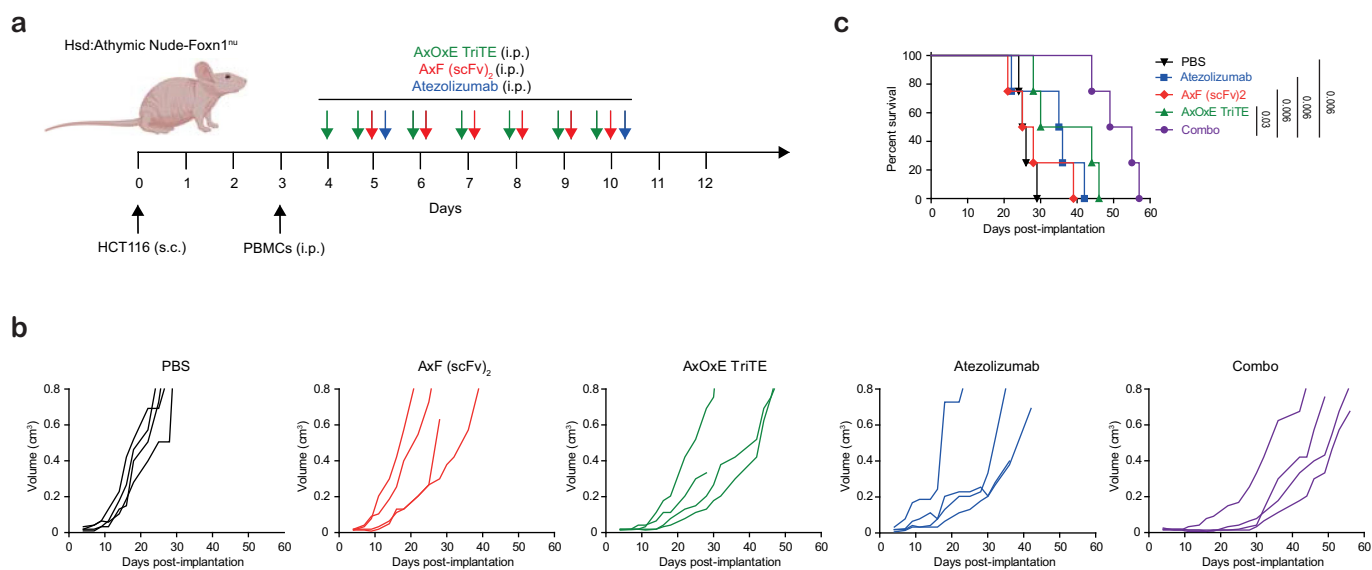


**Figure 5.** *In vivo* antitumor efficacy of EpCAM $\times$ CD3 $\times$ EGFR TriTE enhanced by PD-L1 $\times$ TGF- $\beta$  bispecific antibody. (a) Hsd:Athymic Nude-Foxn1<sup>nu</sup> mice were inoculated subcutaneously with  $2 \times 10^6$  HCT116 tumor cells. When tumors reached 0.3 cm in diameter, mice were randomized into groups ( $n = 4$ /group) and  $10^7$  freshly isolated PBMCs were injected intraperitoneally. PBS, atezolizumab, AxOxE TriTE and/or AxF (scFv)<sub>2</sub> were administered intraperitoneally daily for 6 or 7 d. (b) Tumor volume growth curves for individual mice are represented for each group. (c) Kaplan-Meier survival curves for each treatment group are shown. Overall survival was analyzed with log-rank (Mantel-Cox) test.

EMT markers in TGF- $\beta$ -treated cells. Similarly, blocking of PD-1 binding to PD-L1 was shown as a dose-dependent reversal of luciferase gene repression in Jurkat-PD1 T cells.

Such a construct could be used in combination with T cell-redirecting strategies to prevent immunosuppression of recruited T cells in the TME. Of note, the combination of the AxF (scFv)<sub>2</sub> with TriTE-stimulated PBMC or CAR-T cells

markedly improved *in vitro* the antitumor activity of T cells against colorectal, breast and lung carcinoma cell lines, even though these coculture models without stromal cells are not a perfect correlate of the TME, since they have a profound impact on the biology of both cancer and infiltrating immune cells and can be a major source of TGF- $\beta$  and PD-L1 in the TME. Indeed, we and other have reported that reciprocal

interplay between stromal and cancer cells increases TGF- $\beta$  production in both compartments, even if tumor cells have inactivated the TGF- $\beta$  pathway.<sup>11</sup>

In a hypothetical clinical context, we could presume that administration of AxF (scFv)<sub>2</sub> could be more beneficial than the combination of anti-PD-L1 and anti-TGF- $\beta$  mAb, based on two principles: firstly, the colocalization of the anti-TGF- $\beta$  binding domain to the tumor via PD-L1 targeting would enable the bsAb to block TGF- $\beta$  more efficiently relative to single agent combination; and, secondly, this approach could also ameliorate side effects derived from systemic TGF- $\beta$  inhibition.<sup>10,15</sup> In fact, dual targeting of TGF- $\beta$  and PD-L1 in a single molecule has already been pursued using bifunctional agents, composed of an anti-PD-L1 IgG fused to human TGF- $\beta$  receptor II extracellular domain. Three of them have reached phase clinical trials, bintrafusp alfa (BA) being the first developed.<sup>37</sup> BA inhibited cell proliferation in TGF- $\beta$ -dependent and PD-L1-expressing cells more potently than the TGF- $\beta$  trap or fresolimumab,<sup>38</sup> and enhanced the antitumoral response in murine breast and colon carcinoma models compared to anti-TGF- $\beta$  monotherapy.<sup>39</sup> However, BA phase III clinical trials in NSCLC and biliary tract cancer did not fulfill efficacy endpoints despite preliminary encouraging clinical data. SHR-1701 (retlirafusp alfa) is another bifunctional fusion protein targeting PD-L1 and TGF- $\beta$ , with structure and mechanism of action comparable to those of BA,<sup>40,41</sup> which has demonstrated antitumor activity and safety in phase I study of recurrent or metastatic cervical cancer.<sup>42</sup> In addition, preclinical data of YM101, a tetravalent bispecific TGF- $\beta$  x PD-L1 antibody, have shown better antitumor activity than the combination of anti-TGF- $\beta$  and anti-PD-L1 treatments in several mouse tumor models. Moreover, YM101 effectively overcame anti-PD-L1 resistance in immune-excluded tumor models<sup>43</sup> and, combined with activation of the STING pathway in immune-desert models, promoted T cell infiltration.<sup>44</sup> Its

human counterpart, BiTP<sup>45</sup> or Y101D, is been evaluated in patients with advanced-stage solid tumors (NCT05028556).<sup>28</sup>

Beyond the obvious similarities between BA and SHR-1701, these three agents share their elevated molecular weight, even superior to that of a conventional IgG (172 kDa for BA and 204 kDa for YM101), which can hinder their tumor bioavailability. On the other hand, engineering of smaller antibody fragments has shown to improve tumor uptake rate and intratumoral distribution.<sup>46</sup> In this sense, the AxF (scFv)<sub>2</sub> here described, with a molecular weight of 55 kDa, may offer a competitive advantage in terms of tumor penetration and therefore increased therapeutic effect. Undoubtedly, it comes at the cost of faster clearance, which can be ameliorated using half-life extension strategies, such as fusion to anti-albumin binding domains,<sup>47</sup> albumin fragments<sup>48</sup> or even modifying T cells for endogenous secretion of the AxF (scFv)<sub>2</sub>.<sup>49</sup> Transduction of T cells with the corresponding gene could circumvent the need for continuous antibody administration and enable expression locally at the tumor site. Moreover, the reinvigorating effect of the AxF (scFv)<sub>2</sub> would not be limited to only those cells that have been transduced *ex vivo*, as is the case with CAR-T cells, but wild-type T cells could also benefit from the “bystander” effect. More extensive genetic engineering of CAR-T cells to include a second transgene has been proven viable,<sup>50</sup> enabling CAR-T cells to locally secrete an anti-PD1 scFv<sup>51</sup> or anti-PD-L1 IgG.<sup>52</sup> Similarly, T cells could be engineered to secrete a bi- or tri-specific TCE along with the AxF (scFv)<sub>2</sub>.

Here, we have joined anti-PD-L1 and anti-TGF- $\beta$  binding domains in a single small molecule able to simultaneously disrupt both signaling pathways. The combination of this bsAb with different T cell-based strategies promoted a remarkably superior tumor-specific activation and cytotoxic effect *in vitro* in comparison with untreated CAR-T

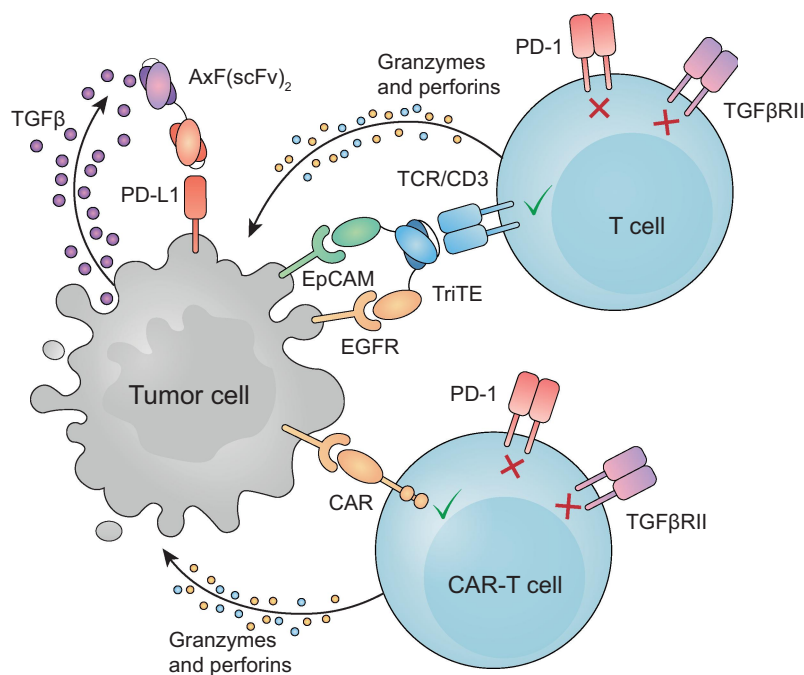


**Figure 6.** Schematic representation of the combined effect of T cell redirection and PD-L1/TGF- $\beta$  blocking. Graphic interpretation of how T cell-mediated lysis of tumor cells is improved in the presence of AxF (scFv)<sub>2</sub>.

cells or wild-type T cells treated only with TriTE (represented in Figure 6). Importantly, *in vitro* results are strongly supported by the increased antitumor response and prolonged survival observed *in vivo*. In conclusion, the AxF (scFv)<sub>2</sub> could be a promising candidate to reverse resistance to immunotherapy in solid tumors. Further studies will be needed to confirm the potential of this combination strategy.

## Abbreviations

bsAb, bispecific antibody; CAR, chimeric antigen receptor; EMT, epithelial mesenchymal transition; ICI, immune checkpoint inhibitor; EGFR, epidermal growth factor receptor; EpCAM, epithelial cell adhesion molecule; HER2, Human epidermal growth factor receptor-2; scFv, single-chain variable fragment; PBMCs, peripheral blood mononuclear cells; PD-L1, Programmed Death-ligand 1; TAA, tumor-associated antigens; TCE, T-cell engager; TGF- $\beta$ , transforming growth factor beta; TME, tumor microenvironment; TriTE, trispecific T-cell engager.

## Acknowledgments

The authors wish to thank donors and Biobank of HUPH/IDIPHISA for the human specimens used in this study.

## Disclosure statement

No potential conflict of interest was reported by the author(s).

## Funding

This study was funded by grants from Carlos III Health Institute [PI19/00132 and PI22/00085], partially supported by the European Regional Development Fund [ERDF] to LS, by grants from the Spanish Ministry of Science and Innovation [PID2020-117323RB-I00 and PDC2021-121711-I00], the Carlos III Health Institute [DTS20/00089], the CRIS Cancer Foundation [FCRIS-2021-0090], the Spanish Association Against Cancer [PROYE19084ALVA and PRYGN234844ALVA], the Fundación “La Caixa” [HR21-00761 project IL7R\_LungCan], and Comunidad de Madrid [P2022/BMD-7225 NEXT\_GEN\_CART\_MAD-CM] to LAV, and Comunidad de Madrid [ANTICIPA-REACT-EU] to JL. ATG was supported by a predoctoral fellowship from Comunidad Autónoma de Madrid [PEJD-2018-PRE/BMD-8314].

## ORCID

Antonio Tapia-Galisteo  <http://orcid.org/0000-0002-0507-8435>  
 Iñigo Sánchez-Rodríguez  <http://orcid.org/0000-0002-6440-0922>  
 Javier Narbona  <http://orcid.org/0000-0002-6118-841X>  
 Patricia Iglesias-Hernández  <http://orcid.org/0000-0002-0815-3322>  
 Anaïs Jiménez-Reinoso  <http://orcid.org/0000-0001-8229-1881>  
 Marta Compte  <http://orcid.org/0000-0002-7138-9266>  
 Patrick Chames  <http://orcid.org/0000-0002-6104-6286>  
 Javier Lacadena  <http://orcid.org/0000-0002-7314-0333>  
 Luis Álvarez-Vallina  <http://orcid.org/0000-0003-3053-6757>  
 Laura Sanz  <http://orcid.org/0000-0002-3119-3218>

## Contributions

Conception and design: LS, ATG. Development of methodology: ATG, ISR, JN, PIH, SAG, AJR, SK, TT. Acquisition, analysis and interpretation of data: ATG, ISR, JN, PIH, LS. Writing, and/or review of the manuscript: ATG, ISR, JN, PIH, SAG, AJR, MC, SK, TT, PC, JL, LAV and LS.

## Data availability statement

The data that support the findings of this study are available from the corresponding author, [LS], upon reasonable request.

## Ethics approval

All procedures involving animals were in accordance with the ethical standards of the corresponding institutional and regional/national committees.

## References

1. Binnewies M, Roberts EW, Kersten K, Chan V, Fearon DF, Merad M, Coussens LM, Gabrilovich DI, Ostrand-Rosenberg S, Hedrick CC, et al. Understanding the tumor immune microenvironment (TIME) for effective therapy. *Nat Med.* 2018;24(5):541–550. doi:10.1038/s41591-018-0014-x.
2. Kennedy LB, Salama AKS. A review of cancer immunotherapy toxicity. *CA Cancer J Clin.* 2020;70(2):86–104. doi:10.3322/caac.21596
3. Mayoux M, Roller A, Pulko V, Sammicheli S, Chen S, Sum E, Jost C, Fransen MF, Buser RB, Kowanetz M, et al. Dendritic cells dictate responses to PD-L1 blockade cancer immunotherapy. *Sci Transl Med.* 2020;12(534):eaav7431. doi:10.1126/scitranslmed.aav7431
4. Ribas A, Wolchok JD. Cancer immunotherapy using checkpoint blockade. *Science.* 2018;359(6382):1350–1355. doi:10.1126/science.aar4060
5. Batlle E, Massagué J. Transforming growth factor- $\beta$  signaling in immunity and cancer. *Immunity.* 2019;50(4):924–940. doi:10.1016/j.immuni.2019.03.024
6. Derynck R, Turley SJ, Akhurst RJ. TGF $\beta$  biology in cancer progression and immunotherapy. *Nat Rev Clin Oncol.* 2021;18(1):9–34. doi:10.1038/s41571-020-0403-1
7. Tauriello DVF, Sancho E, Batlle E. Overcoming TGF $\beta$ -mediated immune evasion in cancer. *Nat Rev Cancer.* 2022;22(1):25–44. doi:10.1038/s41568-021-00413-6
8. Chen B, Mu C, Zhang Z, He X, Liu X. The love-hate relationship between TGF- $\beta$  signaling and the immune system during development and tumorigenesis. *Front Immunol.* 2022;13:891268. doi:10.3389/fimmu.2022.891268
9. Tauriello DVF, Palomo-Ponce S, Stork D, Berenguer-Llargo A, Badia-Ramentol J, Iglesias M, Sevillano M, Ibiza S, Cañellas A, Hernando-Momblona X, et al. TGF $\beta$  drives immune evasion in genetically reconstituted colon cancer metastasis. *Nature.* 2018;554(7693):538–543. doi:10.1038/nature25492
10. Gulley JL, Schlom J, Barcellos-Hoff MH, Wang X-J, Seoane J, Audhuy F, Lan Y, Dussault I, Moustakas A. Dual inhibition of TGF- $\beta$  and PD-L1: a novel approach to cancer treatment. *Mol Oncol.* 2022;16(11):2117–2134. doi:10.1002/1878-0261.13146
11. Navarro R, Tapia-Galisteo A, Martín-García L, Tarín C, Corbacho C, Gómez-López G, Sánchez-Tirado E, Campuzano S, González-Cortés A, Yáñez-Sedeño P, et al. TGF- $\beta$ -induced IGFBP-3 is a key paracrine factor from activated pericytes that promotes colorectal cancer cell migration and invasion. *Mol Oncol.* 2020;14(10):2609–2628. doi:10.1002/1878-0261.12779
12. Mariathasan S, Turley SJ, Nickles D, Castiglioni A, Yuen K, Wang Y, Kadel EE, Koepfen H, Astarita JL, Cubas R, et al. TGF $\beta$  attenuates tumour response to PD-L1 blockade by contributing to exclusion of T cells. *Nature.* 2018;554(7693):544–548. doi:10.1038/nature25501
13. Greco R, Qu H, Qu H, Theilhaber J, Shapiro G, Gregory R, Winter C, Malkova N, Sun F, Jaworski J, et al. Pan-TGF $\beta$  inhibition by SAR439459 relieves immunosuppression and improves antitumor efficacy of PD-1 blockade. *Oncoimmunology.* 2020;9(1):1811605. doi:10.1080/2162402X.2020.1811605
14. Teicher BA. TGF $\beta$ -Directed Therapeutics: 2020. *Pharmacology & Therapeutics.* 2021;217:107666. doi:10.1016/j.pharmthera.2020.107666

15. Morris JC, Tan AR, Olencki TE, Shapiro GI, Dezube BJ, Reiss M, Hsu FJ, Berzofsky JA, Lawrence DP, Perez-Gracia JL. Phase I study of GC1008 (fresolimumab): a human anti-transforming growth factor-beta (TGF $\beta$ ) monoclonal antibody in patients with advanced malignant melanoma or renal cell carcinoma. *PLoS One*. 2014;9(3):e90353. doi:10.1371/journal.pone.0090353
16. Teixeira AF, Ten Dijke P, Zhu H-J. On-target anti-TGF- $\beta$  therapies are not succeeding in clinical cancer treatments: what are remaining challenges? *Front Cell Dev Biol*. 2020;8:605. doi:10.3389/fcell.2020.00605
17. Colak S, Ten Dijke P. Targeting TGF- $\beta$  signaling in cancer. *Trends Cancer*. 2017;3(1):56–71. doi:10.1016/j.trecan.2016.11.008
18. Robbrecht D, Doger B, Grob J-J, Bechter OE, de Miguel MJ, Vieito M, Schadendorf D, Curigliano G, Borbath I, Butler MO, et al. Safety and efficacy results from the expansion phase of the first-in-human study evaluating TGF $\beta$  inhibitor SAR439459 alone and combined with cemiplimab in adults with advanced solid tumors. *J Clin Oncol*. 2022;40(16\_suppl):2524–2524. doi:10.1200/JCO.2022.40.16\_suppl.2524
19. Melisi D, Oh D-Y, Hollebecque A, Calvo E, Varghese A, Borazanci E, Macarulla T, Merz V, Zecchetto C, Zhao Y, et al. Safety and activity of the TGF $\beta$  receptor I kinase inhibitor galunisertib plus the anti-PD-L1 antibody durvalumab in metastatic pancreatic cancer. *J Immunother Cancer*. 2021;9(3):e002068. doi:10.1136/jitc-2020-002068
20. de Miguel M, Umana P, de Moraes AL G, Moreno V, Calvo E. T-cell-engaging therapy for solid tumors. *Clin Cancer Res*. 2021;27(6):1595–1603. doi:10.1158/1078-0432.CCR-20-2448
21. Blanco B, Compte M, Lykkemark S, Sanz L, Alvarez-Vallina L. T cell-redirecting strategies to “STAB” tumors: beyond CARs and bispecific antibodies. *Trends Immunol*. 2019;40(3):243–257. doi:10.1016/j.it.2019.01.008
22. Goebeler M-E, Bargou RC. T cell-engaging therapies — BiTEs and beyond. *Nat Rev Clin Oncol*. 2020;17(7):418–434. doi:10.1038/s41571-020-0347-5
23. Tapia-Galisteo A, Sánchez Rodríguez Í, Aguilar-Sopeña O, Harwood SL, Narbona J, Ferreras Gutierrez M, Navarro R, Martín-García L, Corbacho C, Compte M, et al. Trispecific T-cell engagers for dual tumor-targeting of colorectal cancer. *Oncoimmunology*. 2022;11(1):2034355. doi:10.1080/2162402X.2022.2034355
24. Bargou R, Leo E, Zugmaier G, Klinger M, Goebeler M, Knop S, Noppeney R, Viardot A, Hess G, Schuler M, et al. Tumor regression in cancer patients by very low doses of a T cell-engaging antibody. *Science*. 2008;321(5891):974–977. doi:10.1126/science.1158545
25. Przepiorka D, Ko C-W, Deisseroth A, Yancey CL, Candau-Chacon R, Chiu H-J, Gehrke BJ, Gomez-Broughton C, Kane RC, Kirshner S, et al. FDA Approval: Blinatumomab. *Clin Cancer Res*. 2015;21(18):4035–4039. doi:10.1158/1078-0432.CCR-15-0612
26. Antibody therapeutics approved or in regulatory review in the EU or US. *Antib Soc*. [accessed 2023 Aug 6]. <https://www.antibodysoociety.org/resources/approved-antibodies/>
27. Elshiaty M, Schindler H, Christopoulos P. Principles and current clinical landscape of multispecific antibodies against cancer. *Int J Mol Sci*. 2021;22(11):5632. doi:10.3390/ijms22115632
28. Klein C, Brinkmann U, Reichert JM, Kontermann RE. The present and future of bispecific antibodies for cancer therapy. *Nat Rev Drug Discov*. 2024 Mar 6. doi:10.1038/s41573-024-00896-6
29. Ahn M-J, Cho BC, Felip E, Korantzis I, Ohashi K, Majem M, Juan-Vidal O, Handzhiev S, Izumi H, Lee J-S, et al. Tarlatamab for patients with previously treated small-cell lung cancer. *N Engl J Med*. 2023;389(22):2063–2075. doi:10.1056/NEJMoa2307980
30. Wagner J, Wickman E, DeRenzo C, Gottschalk S. CAR T cell therapy for solid tumors: bright future or dark reality?. *Mol Ther J Am Soc Gene Ther*. 2020;28(11):2320–2339. doi:10.1016/j.ymthe.2020.09.015
31. Maalej KM, Merhi M, Inchakalody VP, Mestiri S, Alam M, Maccalli C, Cherif H, Uddin S, Steinhoff M, Marincola FM, et al. CAR-cell therapy in the era of solid tumor treatment: current challenges and emerging therapeutic advances. *Mol Cancer*. 2023;22(1):20. doi:10.1186/s12943-023-01723-z
32. Khan SA, Joyce J, Tsuda T. Quantification of active and total transforming growth factor- $\beta$  levels in serum and solid organ tissues by bioassay. *BMC Res Notes*. 2012;5(1):636. doi:10.1186/1756-0500-5-636
33. Schmitz KR, Bagchi A, Roovers RC, van Bergen En Henegouwen PMP, Ferguson KM. Structural evaluation of EGFR inhibition mechanisms for nanobodies/VHH domains. *Struct Lond Engl* 1993. 2013;21(7):1214–1224. doi:10.1016/j.str.2013.05.008
34. Sánchez-Martínez D, Baroni ML, Gutierrez-Agüera F, Roca-Ho H, Blanch-Lombarte O, González-García S, Torrebardell M, Junca J, Ramírez-Orellana M, Velasco-Hernández T, et al. Fratricide-resistant CD1a-specific CAR T cells for the treatment of cortical T-cell acute lymphoblastic leukemia. *Blood*. 2019;133(21):2291–2304. doi:10.1182/blood-2018-10-882944
35. Massagué J. Tgfbeta in Cancer. *Cell*. 2008;134(2):215–230. doi:10.1016/j.cell.2008.07.001
36. Narayan V, Barber-Rotenberg JS, Jung I-Y, Lacey SF, Rech AJ, Davis MM, Hwang W-T, Lal P, Carpenter EL, Maude SL, et al. PSMA-targeting TGF $\beta$ -insensitive armored CAR T cells in metastatic castration-resistant prostate cancer: a phase I trial. *Nat Med*. 2022;28(4):724–734. doi:10.1038/s41591-022-01726-1
37. Lan Y, Zhang D, Xu C, Hance KW, Marelli B, Qi J, Yu H, Qin G, Sircar A, Hernández VM, et al. Enhanced preclinical antitumor activity of M7824, a bifunctional fusion protein simultaneously targeting PD-L1 and TGF- $\beta$ . *Sci Transl Med*. 2018;10(424):eaan5488. doi:10.1126/scitranslmed.aan5488
38. Lan Y, Yeung T-L, Huang H, Wegener AA, Saha S, Toister-Achituv M, Jenkins MH, Chiu L-Y, Lazorchak A, Tarcic O, et al. Colocalized targeting of TGF- $\beta$  and PD-L1 by bintrafusp alfa elicits distinct antitumor responses. *J Immunother Cancer*. 2022;10(7):e004122. doi:10.1136/jitc-2021-004122
39. Lind H, Gameiro SR, Jochems C, Donahue RN, Strauss J, Gulley JL, Palena C, Schlom J. Dual targeting of TGF- $\beta$  and PD-L1 via a bifunctional anti-PD-L1/TGF- $\beta$ R agent: status of preclinical and clinical advances. *J Immunother Cancer*. 2020;8(1):e000433. doi:10.1136/jitc-2019-000433
40. Zhang J, Yi J, Zhou P. Development of bispecific antibodies in China: overview and prospects. *Antib Ther*. 2020;3(2):126–145. doi:10.1093/abt/tbaa011
41. Cheng B, Ding K, Chen P, Ji J, Luo T, Guo X, Qiu W, Ma C, Meng X, Wang J, et al. Anti-PD-L1/TGF- $\beta$ R fusion protein (SHR-1701) overcomes disrupted lymphocyte recovery-induced resistance to PD-1/PD-L1 inhibitors in lung cancer. *Cancer Commun Lond Engl*. 2022;42(1):17–36. doi:10.1002/cac2.12244
42. Feng J, Tang D, Wang J, Zhou Q, Peng J, Lou H, Sun Y, Cai Y, Chen H, Yang J, et al. SHR-1701, a bifunctional fusion protein targeting PD-L1 and TGF $\beta$ , for Recurrent or metastatic cervical cancer: a clinical expansion cohort of a phase I study. *Clin Cancer Res*. 2022 Jun 2;28(24):5297–5305. doi:10.1158/1078-0432.CCR-22-0346
43. Yi M, Zhang J, Li A, Niu M, Yan Y, Jiao Y, Luo S, Zhou P, Wu K. The construction, expression, and enhanced anti-tumor activity of YM101: a bispecific antibody simultaneously targeting TGF- $\beta$  and PD-L1. *J Hematol Oncol*. 2021;14(1):27. doi:10.1186/s13045-021-01045-x
44. Yi M, Niu M, Zhang J, Li S, Zhu S, Yan Y, Li N, Zhou P, Chu Q, Wu K. Combine and conquer: manganese synergizing anti-TGF- $\beta$ /PD-L1 bispecific antibody YM101 to overcome immunotherapy resistance in non-inflamed cancers. *J Hematol Oncol*. 2021;14(1):146. doi:10.1186/s13045-021-01155-6
45. Yi M, Wu Y, Niu M, Zhu S, Zhang J, Yan Y, Zhou P, Dai Z, Wu K. Anti-TGF- $\beta$ /PD-L1 bispecific antibody promotes T cell infiltration and exhibits enhanced antitumor activity in triple-negative breast cancer. *J Immunother Cancer*. 2022;10(12):e005543. doi:10.1136/jitc-2022-005543
46. Xenaki KT, Oliveira S, van Bergen En Henegouwen PMP. Antibody or antibody fragments: implications for molecular imaging and targeted therapy of solid tumors. *Front Immunol*. 2017;8:1287. doi:10.3389/fimmu.2017.01287
47. Austin RJ, Lemon BD, Aaron WH, Barath M, Culp PA, DuBridge RB, Evnin LB, Jones A, Panchal A, Patnaik P, et al.



- TriTACs, a novel class of T-Cell-engaging protein constructs designed for the treatment of solid tumors. *Mol Cancer Ther.* **2021**;20(1):109–120. doi:[10.1158/1535-7163.MCT-20-0061](https://doi.org/10.1158/1535-7163.MCT-20-0061)
48. Hangiu O, Compte M, Dinesen A, Navarro R, Tapia-Galisteo A, Mandrup OA, Erce-Llamazares A, Lázaro-Gorines R, Nehme-Álvarez D, Domínguez-Alonso C, et al. Tumor targeted 4-1BB agonist antibody-albumin fusions with high affinity to FcRn induce anti-tumor immunity without toxicity. *iScience.* **2022**;25(9):104958. doi:[10.1016/j.isci.2022.104958](https://doi.org/10.1016/j.isci.2022.104958)
  49. Blanco B, Ramírez-Fernández Á, Bueno C, Argemí-Muntadas L, Fuentes P, Aguilar-Sopeña Ó, Gutierrez-Agüera F, Zanetti SR, Tapia-Galisteo A, Díez-Alonso L, et al. Overcoming CAR-Mediated CD19 downmodulation and leukemia relapse with T lymphocytes secreting anti-CD19 T-cell engagers. *Cancer Immunol Res.* **2022**;10(4):498–511. doi:[10.1158/2326-6066.CIR-21-0853](https://doi.org/10.1158/2326-6066.CIR-21-0853)
  50. Choi BD, Yu X, Castano AP, Bouffard AA, Schmidts A, Larson RC, Bailey SR, Boroughs AC, Frigault MJ, Leick MB, et al. CAR-T cells secreting BiTEs circumvent antigen escape without detectable toxicity. *Nat Biotechnol.* **2019**;37(9):1049–1058. doi:[10.1038/s41587-019-0192-1](https://doi.org/10.1038/s41587-019-0192-1)
  51. Rafiq S, Yeku OO, Jackson HJ, Purdon TJ, van Leeuwen DG, Drakes DJ, Song M, Miele MM, Li Z, Wang P, et al. Targeted delivery of a PD-1-blocking scFv by CAR-T cells enhances anti-tumor efficacy in vivo. *Nat Biotechnol.* **2018**;36(9):847–856. doi:[10.1038/nbt.4195](https://doi.org/10.1038/nbt.4195)
  52. Suarez ER, Chang D-K, Sun J, Sui J, Freeman GJ, Signoretti S, Zhu Q, Marasco WA. Chimeric antigen receptor T cells secreting anti-PD-L1 antibodies more effectively regress renal cell carcinoma in a humanized mouse model. *Oncotarget.* **2016**;7(23):34341–34355. doi:[10.18632/oncotarget.9114](https://doi.org/10.18632/oncotarget.9114)